International Journal of Pharmaceutics 597 (2021) 120337

Contents lists available at ScienceDirect

International Journal of Pharmaceutics

journal homepage: www.elsevier.com/locate/ijpharm

Development of mAb-loaded 3D-printed (FDM) implantable devices based on PLGA

E. Carlier [a,*], S. Marquette [b], C. Peerboom [b], K. Amighi [a], J. Goole [a]

[a] Laboratory of Pharmaceutics and Biopharmaceutics, Université libre de Bruxelles, Faculty of Pharmacy, 1050 Brussels, Belgium
[b] Department of Biological Pharmaceutical Sciences, UCB Pharma S.A, 1420 Braine-l'Alleud, Belgium

ARTICLE INFO

Keywords:
3D printing
Monoclonal antibody
Fused deposition modelling
Implantable systems

ABSTRACT

The main objective of this work was to explore the feasibility to print monoclonal antibody (mAb)-loaded implantable systems using fused-deposition modelling (FDM) to build complex dosage form designs. Indeed, to our knowledge, this work is the first investigation of mAb-loaded devices using FDM. To make this possible, different steps were developed and optimized. A mAb solution was stabilized using trehalose (TRE), sucrose (SUC), hydroxypropyl-β-cyclodextrin (HP-β-CD), sorbitol or inulin (INU) in order to be spray dried (SD). Printable filaments were then made of poly(lactide-co-glycolide) (PLGA) and mAb powder (15% w/w) using hot melt extrusion (HME). The FDM process was optimized to print these filaments without altering the mAb stability. TRE was selected and associated to L-leucine (LEU) to increase the mAb stability. The stability was then evaluated considering high and low molecular weight species levels. The mAb-based devices were well-stabilized with the selected excipients during both the HME and the FDM processes. The 3D-printed devices showed sustained-release profiles with a low burst effect. The mAb-binding capacity was preserved up to 70% following the whole fabrication process. These promising results demonstrate that FDM could be used to produce mAb-loaded devices with good stability, affinity and sustained-release profiles of the mAb.

1. Introduction

Fused-deposition modelling (FDM), a 3D printing (3DP) process, is currently an integral part of the pharmaceutical field (Azad et al., 2020). This technology is an extrusion-based 3DP method that uses heat to melt a thermoplastic polymer filament to build an object in a layer-wise manner. The use of 3DP allows the production of any kind of shape, starting from a digital design (Norman et al., 2017). The emergence of FDM as the most investigated technique for printing drug-delivery systems (DDS) is attributed to its high flexibility, the low cost of the printers and its ability to produce hollow objects (Afrose et al., 2014; Azad et al., 2020). Moreover, the ability of 3DP to complement mass production techniques could be interesting to develop specific DDS in small batches with tailored doses for personalized medicine (Stewart et al., 2020). The main drawback remains the lack of pharmaceutical-grade polymers available to be used in FDM.

However, FDA-approved grade polymers for human use, such as poly (lactic acid) (PLA) and polyvinyl alcohol (PVA), are commonly used as thermoplastic polymers that may be used to make drug-loaded printable filaments (Jamróz et al., 2018). Therefore, numerous academic research efforts have focused on the development of polymeric filaments loaded with different active pharmaceutical ingredients (APIs). Hot melt extrusion (HME) is already widely described, and implemented in the pharmaceutical field to produce such drug-loaded printable filaments (Goyanes et al., 2015b).

HME is based on the melting of polymeric material that is extruded through a die to obtain a homogeneous drug-loaded filament. HME is a solvent-free process that may easily be scaled up (Tiwari et al., 2016). However, this technique is based on the use of relatively high temperatures, which may usually be reduced by adding a plasticizer to decrease the glass transition temperature (T_g) of the polymer. Another alternative to decrease the extrusion temperature could be the use of thermoplastic polymers characterized by a low molecular weight (Fredenberg et al., 2011). Moreover, HME has already been investigated to develop protein-based formulations that were characterized by a controlled release of the loaded API over time (Cossé et al., 2016; Duque et al., 2018; Ghalanbor et al., 2010). Indeed, sustained release allows the number of administrations to be reduced to improve patient compliance as well as to ensure the therapeutic efficacy (Awwad and Angkawinitwong, 2018). Poly(lactide-*co*-glycolide) (PLGA) has been widely investigated and is already a well-known pharmaceutical-grade

* Corresponding author.
E-mail address: emeric.carlier@ulb.be (E. Carlier).

https://doi.org/10.1016/j.ijpharm.2021.120337
Received 15 December 2020; Received in revised form 25 January 2021; Accepted 30 January 2021
Available online 4 February 2021

Abbreviations

3DP	Three-dimensional printing
API	Active pharmaceutical ingredient
BE	Buffer exchange
BCA	Bicinchoninic acid
BSA	Bovine serum albumin
CAD	Computer-aided design
DDS	Drug-delivery system
DSC	Differential scanning calorimetry
ELISA	Enzyme-linked immunosorbent assay
FDM	Fused-deposition modelling
GPC	Gel permeation chromatography
HME	Hot melt extrusion
HMWS	High molecular weight species
HP-β-CD	Hydroxypropyl-β-cyclodextrin
INU	Inulin
LEU	L-leucine
LMWS	Low molecular weight species
M_w	Molecular weight
mAb	monoclonal antibody
OVA	Ovalbumin
PBS	Phosphate buffer solution
PEG	Polyethylene glycol 2000
PLA	Poly(lactic acid)
PLGA	Poly(lactide-co-glycolide) acid
PVA	Polyvinyl alcohol
PVDF	Polyvinylidene fluoride
rpm	Revolutions per minute
SD	Spray dried
SE-HPLC	Size exclusion high-performance liquid chromatography
SOR	Sorbitol
SUC	Sucrose
T_g	Glass transition temperature
TGA	Thermogravimetric analysis
T_{HME}	Hot melt extrusion temperature
T_m	Melting temperature
TRE	D-(+)-trehalose dihydrate
TRE-LEU	Trehalose and L-leucine association
% (w/w)	Weight percentage

polymeric material that is commonly used to make injectable/implantable sustained-release DDS (Cossé et al., 2016; Duque et al., 2018; Ghalanbor et al., 2010). PLGA is a biodegradable and biocompatible polymer approved by the FDA for human use (Lee and Pokorski, 2018). Furthermore, PLGA can be extruded at low temperatures, making it a good candidate for both HME and FDM processes.

For instance, protein-loaded PLGA implants have already been described that use macromolecules such as ovalbumin (OVA) (Duque et al., 2018), bovine serum albumin (BSA) (Cossé et al., 2016) and lysozyme (Ghalanbor et al., 2010). The major challenge that remains is the stabilization of the protein during extrusion. It has been shown that the solid state of the protein could be more advantageous for promoting a higher stability as well as to facilitate its addition into the polymer matrix using the HME process (Cossé et al., 2016; Mensink et al., 2017). However, the protein compounds most often used as models (i.e. OVA, BSA, lysozyme) to produce protein-loaded implants are characterized by low molecular weights in comparison with the conventional biotherapeutic molecules (i.e. immunoglobulin). The interest in and development of monoclonal antibodies (mAbs) have rapidly increased this last decade, leading to a higher attractivity of mAb-based DDS.

Based on the advantages of both technologies (HME and FDM), the interest of producing mAb-loaded filaments using HME and 3DP of devices using FDM technology seems attractive. This would increase the field of FDM-printed devices. This field has been widely investigated to develop oral dosage forms (i.e. tablets, printlets, caplets) or implantable devices (i.e. intrauterine systems) loaded with API such as acetaminophen, indomethacin, aripiprazole or ramipril (Goyanes et al., 2015a; Holländer et al., 2016; Jamróz et al., 2018; Kollamaram et al., 2018).

The novelty of this work was to investigate the ability of FDM technology to print sustained-release mAb-loaded DDS. Indeed, to our knowledge, there is no published paper describing biotherapeutic-loaded DSS made by FDM. This is probably due to HME and FDM both being based on the use of relatively high temperatures, which may be deleterious for the mAb. Therefore, it was necessary to select judiciously the type of thermoplastic polymer to be used and to optimize the manufacturing parameters of both techniques. Furthermore, the formulation of the mAb was investigated to promote its integrity during the processing methods. This was done to obtain a DDS that could allow the stability and the affinity of the loaded mAb to be maintained.

2. Materials and methods

2.1. Materials

PLGA 50:50 lactic acid glycolic acid Resomer® RG502 (7 000–17 000 Da) was purchased from Evonik Industries (Essen, Germany). A humanized monoclonal antibody (mAb) (150 kDa) was provided by UCB Biopharma (Braine-l'Alleud, Belgium). Polyethylene glycol 2000 (PEG 2 kDa) was purchased from Merck Millipore (Massachusetts, USA). Polysorbate 80, D-(+)-trehalose dihydrate (TRE), sucrose (SUC), sorbitol (SOR) and L-leucine (LEU) were purchased from Sigma-Aldrich (Missouri, USA). Inulin (INU) was purchased from Alfa Aesar (Massachusetts, USA). Hydroxypropyl-β-cyclodextrin (HP-β-CD) was purchased from TCI (Tokyo, Japan). Sodium hydroxide beads and dichloromethane were purchased from VWR International (Pennsylvania, USA). Sodium dihydrogen phosphate monohydrate, di-sodium hydrogen phosphate and L-histidine were purchased from Merck Millipore (Massachusetts, USA). A Pierce™ BCA protein assay kit was purchased from Thermo Fisher Scientific (Massachusetts, USA).

2.2. Methods

2.2.1. mAb solution preparation

The solutions of mAb to be spray dried were made from an initial aqueous stock solution (pH 5.6). The mAb formulations were prepared by buffer exchange (BE) using a single Vivaflow 200 cross flow cassette (Sartorius, Germany) equipped with a 30 kDa polyethersulfone membrane, coupled with a Masterflex L/S peristaltic pump (Cole-Parmer, USA). The solvent exchange was performed using a 5:1 v/v ratio compared to the initial volume of mAb in solution. The final solution was filtered on a 0.22-µm membrane using the Stericup® filtration system (Merck KGaA, Germany). The concentration of the mAb in solution was evaluated using a spectrophotometer (Cary 60 UV–Vis, Agilent, USA), equipped with a SoloVPE system (C Technologies Inc, USA), at 280 nm.

2.2.2. Spray drying

The mAb-containing solutions were spray dried using a lab-scale B-290 spray dryer (Büchi Labertechnik, Flawil, Switzerland) equipped with a 0.7 mm nozzle. Settings were based on in-house procedure and kept constant for all formulations. The inlet air temperature was set at 120 °C; the drying air rate at 35 m^3/h; the gas spray flow at 800 L/h; and

the solution feed rate at 3 mL/min. The outlet temperature ranged between 55 and 62 °C. The solutions were prepared in a 15 mM histidine buffer at pH 5.6. An overview of the mAb solution compositions, concentrations and mAb:stabilizer ratios is shown in Table 1. All powders were sealed in a polypropylene container and stored in a desiccator under vacuum.

2.2.3. Hot melt extrusion

Printable filaments were prepared from physical mixtures of raw PLGA, PEG 2 kDa and mAb-containing SD powders which were previously blended together using a Turbula® mixer (Willy A. Bachofen AG, Muttenz, Switzerland) (67 rpm, 30 min). The blend was manually fed into a 11-mm twin screw extruder (Process-11, Thermo Fischer Scientific, Massachusetts, USA), equipped with modular screws (length to diameter ratio 40:1), and a round die with a diameter of 1.6 mm. The barrel was heated using a temperature gradient controlled by eight thermocouples. The feeding zone was maintained at room temperature using a water circulator. The three first segments were set at 20, 40 and 80 °C, respectively. The middle segments, from the 4th to 6th thermocouple, were set at 90 °C. The last thermocouple, which was located immediately before the die, was set at 85 °C and the die itself was set at 75 °C. For all experiments, the screw speed was set at 40 rpm during the feeding and 60 rpm when the filament was manually coiled. These parameters were kept constant (Table 1).

2.2.4. 3D printing of mAb-loaded devices

The design of the devices was drawn using the 3D computer-aided design (CAD) software ThinkerCAD™ (AutoDesk® Inc., USA) and exported as an .stl file (Fig. 1a). Then, the .stl file was imported into open-source software, Slic3r 1.3.0., for slicing and was converted to a .gcode file. The dimensions of the devices were 20 × 5 × 2 mm (length, width, height) for a volume of 178.43 mm^3.

A Hyrel 3D system 30 M printer (GA, USA), equipped with a 0.5 mm MK2-250 hot extruder, was used to print the mAb-loaded devices. The temperature of the build platform did not need to be controlled. The printing temperature was set at 105 ± 2 °C. The printing speed was set at 1 mm/s for the first layer and 10 mm/s for the others. The layer thickness of the devices was set at 0.1 mm and 0.3 mm to evaluate its influence on the potential degradation of the loaded mAb as well as on its release profile. The printing of devices was performed with an infill of 100% (v/v).

2.2.5. Differential scanning calorimetry

Thermal analyses of SD powders, printable filaments and 3DP DDS were performed with differential scanning calorimetry (DSC) using a heat-flux type DSC Q2000 (TA instruments, Delaware, USA) equipped with a cooling system. Nitrogen was used as the purge gas (flow rate = 50 mL/min) and data were collected with TA Instruments® Trios 4.5.0 software. Samples of 5–10 mg were introduced into TA aluminium pans and sealed with a lid (Tzero) made of the same material to evaluate the thermal properties (e.g. T_g determined at the midpoint of the transitions and the melting temperature (T_m)) of the filaments as well as of the 3DP devices. The reference consisted of an empty sealed pan. During the first cycle, the oven was heated from −50 °C to 150 °C at 10 °C/min. During the second cycle, the samples were cooled to −50 °C before being heated again to 150 °C at 10 °C/min.

2.2.6. Thermogravimetric analysis

Thermogravimetric analysis (TGA) were performed on a Q500 TGA (TA Instruments, Delaware, USA), equipped with a balance with a sensitivity of 0.1 μg. Nitrogen was used as the purge gas (flow rate = 60 mL/min.). Samples of 5–8 mg were loaded into platinum pans to assess the thermal stability of plasticizers and polymers. The climatic chamber was heated at 10 °C/min from 30 °C to 600 °C. Data collection and analysis were performed using TA Instruments® Trios 4.5.0 software.

2.2.7. mAb stability evaluation

The quantification of the mAb monomer as well as the evaluation of high molecular weight species (HMWS) and low molecular weight species (LMWS) contents was carried out by size exclusion high-performance liquid chromatography (SE-HPLC). This analysis was conducted on samples obtained either from dissolution studies or after extraction from the printable filaments and 3DP devices. These quantifications were performed on an Agilent 1200 series LC system equipped with a UV detector (Agilent Technologies, Waldbronn, Germany). A TSK Gel G3000 SWXL column of 7.8 mm ID × 30.0 cm length (Tosoh Bioscience GMBH, Stuttgart, Germany) with a TSK Gel BioAssist SWXL 6.0 mm × 4.0 cm guard column (Tosoh Bioscience GMBH, Stuttgart, Germany) was used with a flow rate set at 1.0 mL/min; an injection volume at 50 μL; and a wavelength at 280 nm. The mobile phase was a phosphate buffer solution (PBS) 0.2 M at pH 7.0. The stability of the mAb was evaluated using the percentage of monomer loss, which corresponded to the difference in the percentage of monomers before and after the HME and 3DP processes. Monomer, HMWS and LMWS levels (%) were compared to a reference of the mAb solution obtained after BE.

2.2.8. mAb extraction from the polymeric matrix

To evaluate the stability of mAb melt-encapsulated in printable filaments and in 3D-printed devices, samples of approximatively 10 mg were placed in Nanosep® centrifugal devices with 0.2 μm Bio-Inert® membrane (Pall, New-York, USA) and dissolved in 0.5 mL of dichloromethane. The Nanosep® devices were stirred at 600 rpm for 2 h at room temperature to dissolve the PLGA, using a Thermomixer® comfort tube mixer (Eppendorf AG, Hamburg, Germany). The samples were centrifuged at 12 000 rpm for 10 min and the medium was withdrawn. Then, 0.5 mL of dichloromethane were added again. The sample was stirred for 5 min and centrifuged as previously mentioned. This step was repeated twice. Dichloromethane was removed and the Nanosep® devices containing the mAb precipitate were placed for 1 h under vacuum to remove potential residual solvent. Then, 0.5 mL of PBS (0.2 M, pH 7.0) containing 0.02% w/w of polysorbate 80 (PS80) were added into the tube to solubilize the mAb before the solution was stirred at 600 rpm for 2 h. The Nanosep® devices were then centrifuged for 10 min at 12 000 rpm (adapted from Arrighi et al., 2019). The mAb stability was then evaluated by SEC (as described in Section 2.2.7).

2.2.9. mAb loading after melt encapsulation

The amount of mAb encapsulated into the PLGA matrix was determined using colorimetric detection by bicinchoninic acid (BCA) protein assay. Briefly, samples (printable filament and 3DP devices) of approximatively 200 mg were dissolved in 50 mL of sodium hydroxide solution (0.1 M, pH 12.8) for 5 h and stirred at 300 rpm, at room temperature. The solutions were filtered on 0.45 μm polyvinylidene fluoride (PVDF) Acrodisc® syringe filters (Pall, Saint-Germain-en-Laye, France). Then, the Pierce™ microplate procedure was carried out to determine the amount of melt-encapsulated mAb. The quantification of standards and samples was performed at 562 nm on a SpectraMax M5 microplate reader (Molecular Devices, California, USA) at room temperature. Overall, the mAb loading was determined as follows:

$$mAb\ loading\ (\%) = \frac{\text{amount of melt} - \text{encapsulated mAb}}{\text{amount of 3DP device}} * 100 \quad (1)$$

Eq. (1). mAb loading (%) after melt-encapsulation.

2.2.10. Dissolution studies

To evaluate the release profiles of the loaded mAb from 3DP DDS, *in vitro* dissolution studies were performed. 3DP devices (~200 mg) were placed in 5 mL Eppendorf® tube filled with 5 mL of PBS (0.2 M, pH 7.0, 37 °C). These were then stirred at 600 rpm using a Thermomixer® comfort tube mixer (Eppendorf AG, Hamburg, Germany) (adapted from (Marquette et al., 2014)). At predetermined times, 5 mL of medium were withdrawn, collected and filtrated on 0.45 μm PVDF Acrodisc® syringe

Table 1
Theoretical composition of evaluated mAb formulations for SD batches (% w/V), solid composition of SD powders (% w/w), printable filaments produced using HME batches (% w/w) and associated 3DP batches with layer thickness of 0.1 mm and 0.3 mm.

SD batch number	Stab.	mAb:stab. ratio	liquid composition (% w/V) - after BE				Solid composition (% w/w) - after spray drying				HME batch number	RG502 (% w/w)	PEG (% w/w)	Excipient (% w/w)	mAb (% w/w)	3DP 0.1 mm batch number	3DP 0.3 mm batch number
			HIS	Stab.	LEU	mAb	HIS	Stab.	LEU	mAb							
SD_1	SUC	1.5:1	0.2	5.1	–	8.0	1.7	38.3	–	60.0	HME_1	60.1	6.6	13.3	20.0	–	–
SD_2		2.0:1	0.2	3.8	–	8.0	1.9	31.4	–	66.7	HME_2	62.9	6.9	10.1	20.1	–	–
SD_3		2.5:1	0.2	3.2	–	8.0	2.1	26.5	–	71.4	HME_3	64.1	7.1	8.7	20.2	–	–
SD_4	TRE	1.5:1	0.2	5.1	–	8.0	1.7	38.3	–	60.0	HME_4	60.1	6.6	13.3	20.0	–	–
SD_5		2.0:1	0.2	3.8	–	8.0	1.9	31.4	–	66.7	HME_5	62.9	6.9	10.1	20.1	–	–
SD_6		2.5:1	0.2	3.2	–	8.0	2.1	26.5	–	71.4	HME_6	64.1	7.1	8.7	20.2	–	–
SD_7	SOR	1.5:1	0.2	5.1	–	8.0	1.7	38.3	–	60.0	HME_7	60.1	6.6	13.3	20.0	–	–
SD_8		2.0:1	0.2	3.8	–	8.0	1.9	31.4	–	66.7	HME_8	62.9	6.9	10.1	20.1	–	–
SD_9		2.5:1	0.2	3.2	–	8.0	2.1	26.5	–	71.4	HME_9	64.1	7.1	8.7	20.2	–	–
SD_10	INU	1.5:1	0.2	5.1	–	8.0	1.7	38.3	–	60.0	HME_10	60.1	6.6	13.3	20.0	–	–
SD_11		2.0:1	0.2	3.8	–	8.0	1.9	31.4	–	66.7	HME_11	62.9	6.9	10.1	20.1	–	–
SD_12		2.5:1	0.2	3.2	–	8.0	2.1	26.5	–	71.4	HME_12	64.1	7.1	8.7	20.2	–	–
SD_13	HP-	1.5:1	0.2	5.1	–	8.0	1.7	38.3	–	60.0	HME_13	60.1	6.6	13.3	20.0	–	–
SD_14	β-CD	2.0:1	0.2	3.8	–	8.0	1.9	31.4	–	66.7	HME_14	62.9	6.9	10.1	20.1	–	–
SD_15		2.5:1	0.2	3.2	–	8.0	2.1	26.5	–	71.4	HME_15	64.1	7.1	8.7	20.2		
SD_16	SUC	2.0:1	0.2	3.8	–	8.0	1.9	31.4	–	66.7	HME_16	69.4	7.6	7.6	15.3	3DP_1	3DP_2
SD_17	SUC-LEU	2.0:1	0.2	3.2	0.6	8.0	1.9	26.4	5	66.7	HME_17	69.4	7.6	7.6	15.3	–	3DP_3
SD_18	TRE	2.0:1	0.2	3.8	–	8.0	1.9	31.4	–	66.7	HME_18	69.4	7.6	7.6	15.3	3DP_4	3DP_5
SD_19	TRE-LEU	2.0:1	0.2	3.2	0.6	8.0	1.9	26.4	5	66.7	HME_19	69.4	7.6	7.6	15.3	–	3DP_6
SD_20	TRE-LEU	2.0:2	0.2	3.2	0.6	8.0	1.10	26.5	6	66.8	HME_20	69.4	7.6	7.6	15.3	–	3DP_7

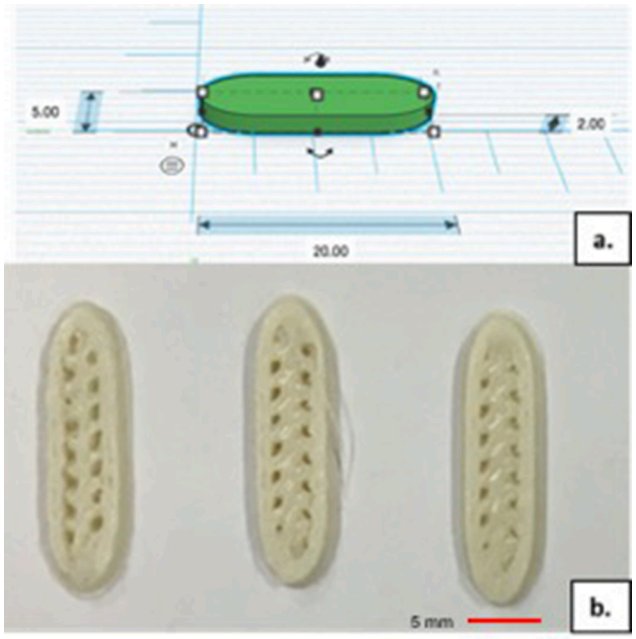

Fig. 1. a. Implantable device (20 × 5 × 2 mm (L × W × H)) designed with TinkerCad™. **b.** 3Dprinted devices (100% (w/w)) obtained using the Hyrel 30 M system.

filters (Pall, Saint-Germain-en-Laye, France). A similar volume was replaced with fresh buffer (5 mL). The filtrated solutions were measured using SEC equipped with a UV-detector at 280 nm (as described in Section 2.2.7) and analysed for pH (pH-meter, Mettler-Toledo, USA).

2.2.11. PLGA degradation during dissolution studies

Quantification of the decrease in PLGA in polymer molecular weight (Mw) during the drug release was carried out using gel permeation chromatography (GPC). The protocol was similar to that used for the dissolution test. At predetermined times, the 3DP devices were withdrawn and dried under vacuum for 24 h. The samples of 5 mg were dissolved in chloroform and GPC analysis was performed in an Agilent 1200 series LC system equipped with an Agilent DRI refractive index detector and three columns: a PL gel 5 mm guard column (Polymer Laboratories® Ltd., UK) and two PL gel Mixed-B 5 μm columns (columns for separation of polystyrene with a Mw ranging from 200 to 4×10^5 g/mol). Chloroform was used as the mobile phase at a flow rate of 1 mL/min at 30 °C. Molecular weights were calculated using polystyrene standards.

2.2.12. Enzyme-linked immunosorbent assay (ELISA test)

The binding capacity of the mAb was assessed using an ELISA test that was developed for the targeted mAb. The data were expressed as a percentage of sample concentration spectrophotometrically determined at 280 nm. Briefly, a 96-well plate was coated overnight at room temperature with a goat anti-human target antibody. Then, the plate was blocked using a solution containing bovine serum albumin to reduce the non-specific binding. The compound targeted by the goat anti-human target antibody was added to the medium. The samples containing the mAb were added to the 96-well plate. The bounded mAb was detected using horseradish peroxidase (HRP)-conjugated goat IgG fraction to human kappa light chain (MP Biomedicals, USA), and the reaction was visualized after the addition of chromogenic tetramethylbenzidine substrate (TMB substrate, Bio-Rad, USA). The colour development was stopped after 15 min with 0.5 N sulfuric acid and the absorbance values (proportional to the amount of protein in the medium) were measured at 450 nm and with 655 nm background compensation on a Spectramax M5 microplate reader (Molecular Devices, USA). All incubation steps were performed at room temperature and the plates were continuously shaken.

2.2.13. Data analysis

All experiments were performed in triplicate, unless otherwise specified. Prism 8 software (GraphPad software, USA) was used for statistical analysis. The results are expressed as a mean ± standard deviation. Statistical significance was determined at p-value < 0.05 using ANOVA and Tukey's or Dunnett's post-hoc test (as recommended by Prism software).

3. Results and discussion

Initially, the mAb solution was formulated with different stabilizers. These solutions were spray dried to produce mAb-loaded powders. Indeed, it was necessary to stabilize mAb in solid state to increase its stability and to facilitate handling during further processing. Then, a physical mixture of mAb-loaded SD powder, RG502 and PEG was extruded using HME to produce printable filaments. These printable filaments were used to feed the 3DP printer and to print our devices. The selection of the optimal formulation was carried out by evaluating mAb integrity after each manufacturing steps (spray drying, HME, 3DP). Finally, *in vitro* evaluations (dissolution test and binding capacity) were performed.

3.1. Preliminary study on raw materials and printable filaments

The thermal properties, including their degradation temperature, of all raw materials were assessed using DSC and TGA analysis, respectively.

The TGA thermograms of the SD mAb powder showed a slight weight loss (~4% w/w) when a temperature of 100 °C was reached. Such decrease could be attributed to the residual moisture content in the SD mAb powder. Indeed, the mean residual moisture in the SD powders was found to be 3.4 ± 0.8%. No further drying was performed to reduce the residual moisture but the storage of the mAb-loaded SD powders was carried out in a desiccator under vacuum. It may be interesting to compare these results using Karl Fisher titration in further investigations. A second weight loss was observed above 150 °C on all the SD mAb-loaded powders. Therefore, it seemed that the mAb-loaded powders could ensure the stability of the mAb during both HME and 3DP. However, the assessment of the secondary and the tertiary structure of mAb was out of the scope of this study. It is important to note that the processes reached maximum temperatures of 90 and 105 °C, respectively.

In addition, the degradation temperature of raw RG502 was around 175 °C. Moreover, it was observed that no apparent weight loss appeared under 200 °C for raw PEG and for the extruded filaments loaded with mAb. No residual moisture was observed in RG502 and PEG raw materials. These results confirmed that all raw materials seemed stable and may be processed according to the temperatures in both HME and 3DP (90 °C and 105 °C, respectively). Indeed, only the mass loss was characterized using TGA. Other methods were required to state the mAb stability, such as SEC and binding capacity.

DSC analyses were then carried out to evaluate the influence of the addition of PEG and mAb-loaded SD powder on the T_g of the thermoplastic polymer RG502. Indeed, as the aim of this work was to develop mAb-loaded 3DP DDS, the T_g should be as low as possible to allow the temperature of the different processes (HME, 3DP) and the potential degradation of the biotherapeutic as a consequence, to be decreased.

The T_g of RG502 was found to be 38.0 ± 0.7 °C, which was consistent with data already described in literature (Pignatello et al., 2009). PEG was characterized by a sharp endothermic peak at 52 °C. The T_g of RG502 decreased to 21.8 ± 0.4 °C when PEG and SD powder were added during HME (data not shown). Such decrease in the T_g, in addition to the loss of the sharp melting peak of PEG, demonstrated that mAb-loaded SD

powder and PEG were properly dispersed in the molten polymer matrix (Zhang et al., 2017). This step was mandatory to ensure the further physical stability of the system before any other investigations. It is widely accepted that miscibility between polymer–polymer, polymer-API or amorphous mixtures of APIs was related to a unique T_g value (Luebbert et al., 2017; Shah et al., 2013).

3.2. Formulation screening and mAb stability after the spray-drying process

Stabilizers were selected to maintain mAb integrity during all the manufacturing steps. The main deleterious factor was the relatively high temperatures that were used during both HME and 3DP. It is widely accepted that stabilizers such as sugars or polyols are effective excipients for stabilizing mAb during spray drying (Mensink et al., 2017). The solid state improves thermal stress resistance, shear-induced denaturation and surface adsorption instabilities (Ohtake et al., 2011). Unfortunately, the choice of stabilizer is not universal and needs to be adapted to each biotherapeutic with regard to the stress factors associated with the process (Le Basle et al., 2020; Wang et al., 2007).

SUC, TRE, HP-β-CD, SOR and INU are commonly used in mAb formulations in solid state (Baek et al., 2017; Bowen et al., 2013; Gidwani and Vyas, 2015; Kanojia et al., 2016; Maury et al., 2005). It was interesting to implement a wide approach using different types of stabilizer classified as disaccharides (SUC, TRE), cyclic oligosaccharides (HP-β-CD), polysaccharides (INU) and polyols (SOR) (Cummings and Stephen, 2007). Stabilizers are able to form H-bonds with proteins, which leads to water replacement. Moreover, they are able to form a matrix around the protein to reduce or prevent its mobility. This well-known effect is called “vitrification theory” (Mensink et al., 2017).

The effect of the addition of stabilizers on the stability of the loaded mAb was investigated using three different mAb:stabilizer ratios (1.5:1, 2.0:1 and 2.5:1) (Table 1). A mAb:stabilizer ratio of 2.0:1 was previously described as increasing the stability of mAb during a spray-drying process (Bowen et al., 2013). Higher and lower ratios were also investigated to evaluate their influence on the stability of our own mAb, which was successively stressed by heat through HME and 3DP.

The mAb formulation was performed using BE and no instabilities were demonstrated between the initial mAb solution and the BE step. The percentage of HMWS after BE was similar to that observed from the mAb reference solution (2.6 ± 0.4%) (Table 2).

After SD, there was no significant formation of HMWS for mAb:stabilizer ratios of 1.5:1 and 2.0:1, regardless of the nature of the stabilizer (p-value > 0.05) (Fig. 2). In contrast, when a ratio of 2.5:1 was used, the percentage of HMWS was increased after the SD process, regardless of the nature of the stabilizers, except for SUC and TRE (p-value > 0.05) (Table 2). Indeed, disaccharides such as SUC and TRE may create a more viscous glassy matrix to protect protein molecules (Jain and Roy, 2009; Kamerzell et al., 2011). Following these results, the 2.5:1 ratio was discarded. Moreover, as ratios of 1.5:1 and 2.0:1 showed similar results, the 2.0:1 ratio allowed a higher proportion of mAb versus stabilizers and was selected for further investigations (Table 2).

The LMWS level was also assessed and no fragmentation was observed on the raw mAb. A similar observation was made after BE and SD, regardless of the mAb:stabilizer ratio (Table 2).

3.3. Extrusion of mAb-loaded printable filaments

All filaments were successfully prepared, with a diameter between 1.70 and 1.75 mm as recommended to feed the FDM 3D printer (Melocchi et al., 2015).

At the beginning, several trials were performed using a mAb loading of 20% (w/w) in the filaments. Using this percentage, a high amount of mAb was required and it was observed that such high loading tended to increase the burst effect due to percolation issues. This effect occurred as the PLGA matrix was not able to sustain the release of the loaded mAb within the first hours of dissolution (Bode et al., 2019; Ghalanbor et al., 2012). Therefore, the loading percentage was progressively decreased. It was shown that the maximal percentage that allowed minimal degradation of the mAb, optimal homogeneity within the filament and minimal burst effect from the 3DP devices was a loading of 15% (w/w).

Afterwards, the mAb-loaded SD powder was mixed with PLGA and PEG and extruded to make printable filaments. It was shown that the percentage of HMWS was increased due to the use of relatively high temperatures, regardless the nature of the stabilizer (p-value < 0.0001).

However, it was demonstrated that the percentage of HMWS reached 6.4 ± 0.2%, 11.2 ± 0.5% and 4.9 ± 0.1% when HP-β-CD (HME_14), SOR (HME_8) and INU (HME_11) were added to the formulations (mAb:stabilizer ratio 2.0:1) (Fig. 2). In contrast, SUC and TRE seemed the most adapted to stabilizing the mAb during the HME process performed at 90 °C. Indeed, the percentages of HMWS only increased to 3.3 ± 0.3% (SUC, HME_2) and 3.8 ± 0.5% (TRE, HME_5), respectively (Fig. 2). No significant difference was highlighted for both disaccharides after the HME process (p-value > 0.05).

In addition, the percentage of LMWS was evaluated after HME (Table 2). It was observed that fragmentation appeared when HP-β-CD and SOR were added to the formulations (Table 2). In contrast, no LMWS were shown with SUC, TRE and INU (Table 2). The fragmentation was induced when high temperatures were used. Indeed, non-enzymatic reactions could lead to the fragmentation of disulphide or peptide bonds, specifically in the hinge region. Furthermore, high temperatures can promote deamidation of amino acids such as asparagine and glutamine. This phenomenon is accelerated at acidic pH (Le Basle et al., 2020; Nowak et al., 2017).

Nevertheless, these results showed that a higher HMWS level was observed when a higher temperature and a longer residence time were

Table 2
Comparison of HMWS and LMWS levels of mAb formulation (mAb:stabilizer ratios: 1.5:1; 2.0:1 and 2.5:1) after BE and HME. The monomer content as well as the HMWS and LMWS levels of the mAb reference are shown.

mAb:stabilizer ratio		1.5:1			2.0:1			2.5:1		
Stabilizer	Process	BE	SD	HME	BE	SD	HME	BE	SD	HME
SUC	HMWS (%)	2.5	2.7 ± 0.3	3.2 ± 0.2	2.5	2.8 ± 0.1	3.3 ± 0.3	2.9	3.51 ± 0.04	4.2 ± 0.2
	LMWS (%)	0.0	0.0 ± 0.0	0.0 ± 0.0	0.0	0.0 ± 0.0	0.0 ± 0.0	0.0	0.0 ± 0.0	0.0 ± 0.0
TRE	HMWS (%)	2.5	2.8 ± 0.8	3.2 ± 0.5	2.8	3.2 ± 0.5	3.8 ± 0.5	2.9	3.54 ± 0.02	4.3 ± 0.1
	LMWS (%)	0.0	0.0 ± 0.0	0.0 ± 0.0	0.0	0.0 ± 0.0	0.0 ± 0.0	0.0	0.0 ± 0.0	0.0 ± 0.0
SOR	HMWS (%)	2.3	3.1 ± 0.1	14.6 ± 0.5	2.5	3.3 ± 0.2	11.2 ± 0.4	2.4	3.22 ± 0.03	8.9 ± 0.3
	LMWS (%)	0.0	0.0 ± 0.0	0.0 ± 0.0	0.0	0.0 ± 0.0	0.4 ± 0.1	0.0	0.00 ± 0.01	0.2 ± 0.1
INU	HMWS (%)	2.5	3.7 ± 0.2	5.4 ± 0.2	2.5	3.6 ± 0.3	4.9 ± 0.1	2.6	4.05 ± 0.02	4.8 ± 0.1
	LMWS (%)	0.0	0.0 ± 0.0	0.0 ± 0.0	0.0	0.0 ± 0.0	0.0 ± 0.0	0.0	0.0 ± 0.0	0.0 ± 0.0
HP-β-CD	HMWS (%)	2.8	3.0 ± 0.3	9.4 ± 0.8	2.5	3.5 ± 0.5	6.3 ± 0.2	2.8	4.10 ± 0.02	8.0 ± 0.5
	LMWS (%)	0.0	0.0 ± 0.0	0.0 ± 0.0	0.0	0.0 ± 0.0	0.10 ± 0.05	0.0	0.02 ± 0.01	0.23 ± 0.02
mAb reference solution	Monomer (%)	97.4 ± 0.4								
	HMWS (%)	2.6 ± 0.4								
	LMWS (%)	0.0 ± 0.0								

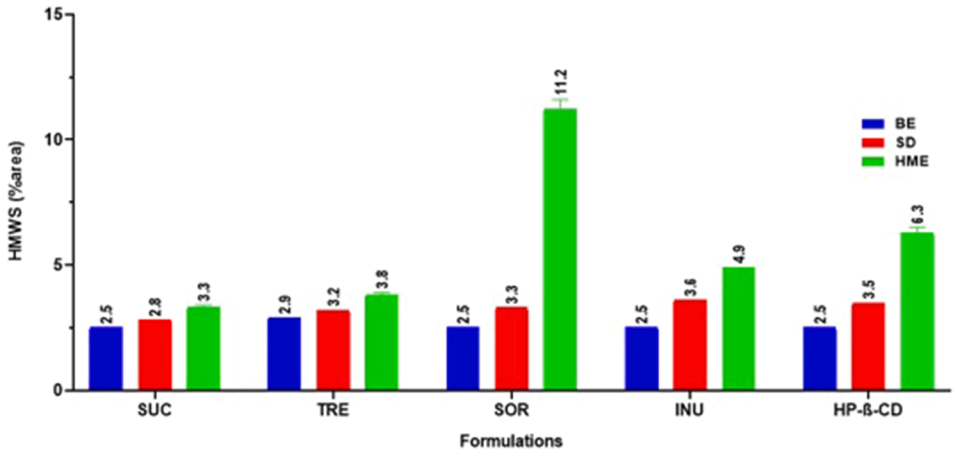

Fig. 2. Comparison of the HMWS levels for the mAb formulation (mAb: stabilizer ratio 2.0:1) containing SUC, TRE, HP-β-CD, SOR and INU after BE, spray drying and HME. Formulations are summarized as SUC: SD_2 (BE, SD), HME_2 (HME); TRE: SD_5 (BE, SD), HME_5 (HME); SOR: SD_8 (BE, SD), HME_8 (HME); INU: SD_11 (BE, SD), HME_11 (HME); HP-β-CD: SD_14 (BE, SD), HME_14 (HME) (Table 1).

used. This effect was regardless of the addition of stabilizers. It could be due to the inability of SOR to promote mAb stability during transfer of heat. In the literature, SOR was used to stabilize mAb in solution or during a freeze-drying process. However, aggregation was promoted due to the recrystallization of SOR during storage (Kamerzell et al., 2011; Piedmonte et al., 2015). Crystallization may lead to a loss of protein-stabilizer interactions (Mensink et al., 2017). There could be a similar effect during HME where enough energy was provided to SOR to recrystallize and thus promote the degradation of the mAb. However, no X-ray diffraction was performed to support these data.

HP-β-CD and INU were less effective at maintaining mAb stability during HME in comparison to the other stabilizers (SUC and TRE). HP-β-CD has been reported to interact with proteins via the hydroxypropyl functions (Serno et al., 2011). Instabilities could be due to the lack of interactions between mAb and CD. INU is a polysaccharide with a higher Mw, where steric hindrance and reduced flexibility may lead to reduced interactions between INU and mAb (Tonnis et al., 2015). According to the evaluation of HMWS and LMWS levels, the mAb integrity was ensured during HME using TRE and SUC as stabilizers (Table 2).

Overall, SUC and TRE seemed to be the most suitable stabilizers for stabilizing the formulations over the successive production steps (i.e. BE, spray-drying and HME). Interestingly, both compounds are characterized by similar structure, which belongs to disaccharide class. It has already been noted that such derivatives are able to create hydrogen bonds with the protein. They also form a glassy matrix to avoid protein–protein interactions, which are known to promote aggregation issues. The glassy matrix was ensured with high T_g values of both SUC (60 °C) and TRE (120 °C) (Cicerone et al., 2015; Jain and Roy, 2009; Maury et al., 2005; Mensink et al., 2017; Rajagopal et al., 2013).

Finally, the mAb loading was assessed on the printable filaments before the printing process. This showed that the loadings of all the filaments were similar to the theoretical loading (15% w/w), with very low standard deviations (Table 3). These results indicated that the manufacturing process was suitable and reproducible to produce uniform printable filaments with homogeneous dispersion.

Table 3
mAb loading in printable filaments and 3DP devices obtained by BCA assay.

HME batch name	mAb loading (% w/w)	3D batch name	mAb loading (% w/w)
HME_16	16.0 ± 0.1	3DP_2	15.8 ± 0.2
HME_17	15.2 ± 0.1	3DP_3	15.1 ± 0.2
HME_18	16.2 ± 0.1	3DP_5	16.2 ± 0.3
HME_19	15.6 ± 0.2	3DP_6	15.5 ± 0.2
HME_20	15.9 ± 0.5	3DP_7	15.5 ± 0.5

3.4. 3DP of the mAb delivery devices

Slicing software was used to design a model of 3DP DDS with a shape that could be implantable. The use of cylindrical shapes is commonly reported for the development of implantable DDS. As 3DP is a relatively new process in pharmaceutical field, techniques such as HME and electrospinning have been widely investigated to produce cylindrical implants (Cossé et al., 2016; Duque et al., 2018; Lee and Pokorski, 2018). Indeed, HME is able to produce rod (cylindrical)- or film-based shapes depending on the shape of the die. In the literature, 3DP implants have been designed using the Etonogestrel-implant developed by Merck as a reference. The development of the cylindrical DDS was characterized by a diameter of 2 mm and a length of 40 mm (Stewart et al., 2020). The main advantage of 3DP is its versatility and its ability to produce any shape related to the selected design. Then, 3DP allows the production of devices in a layer-wise manner with a high control of the deposition (e.g. height of the layers). Furthermore, FDM technology is performed to build devices without any post-processing step (Pietrzak et al., 2015).

The printing process was performed in a room at 20 °C. Indeed, the physical state of the filaments may be quickly modified due to the temperature as their T_g is around 22 °C, as previously mentioned. Therefore, at 20 °C, filaments were able to be printed as their stiffness was preserved. However, the handling of the filaments induced a heat transfer by conduction. This phenomenon was greater when the filaments were loaded in the print head. Indeed, they were too soft to travel along the feeding gears (Costa et al., 2015). To limit these issues, 3DP had to be performed using a "flexible hot flow" MKE-250 modular printing head.

The DDS resolution was macroscopically evaluated and, when the infill was set at 100%, a fully solid DDS was expected. The resolution was the fidelity between the initial CAD files (design) and the 3DP devices, which depends on the FDM technique and printed material (Ligon et al., 2017). Immediate visualization showed defects and a lack of matter at the top of the devices (Fig. 1b). The Hyrel 30 M 3D printer works with a fixed print head and a mobile build platform. The hypothesis was that the platform motion represented the limitation of the process, especially when small pieces were built. The printing step was performed with a printing speed of 1 mm/s for the first layer and of 10 mm/s for the following layers to improve the resolution of DDS. Reducing the printing speed at 1 mm/s ensured a higher adhesion of the first layer on the build platform.

Extraction of mAb was performed on 3DP DDS to evaluate the percentage of both HMWS and LMWS. As mentioned above, SUC and TRE were able to stabilize the mAb during the SD and HME processes. 3DP

was performed at 105 °C, which was the temperature at which adhesion to the build platform and between successive layers was promoted. Layer thicknesses of 0.1 mm and 0.3 mm were evaluated.

Compared to after HME, the percentage of HMWS increased following 3DP, regardless of the layer height or the nature of the disaccharide (Fig. 3). However, it was significantly higher when a layer thickness of 0.1 mm was used (p-value < 0.0001 and p-value < 0.0004, respectively). For instance, the HMWS percentage increased from 3.3 ± 0.1% (HME_16) and 3.8 ± 0.1% (HME_18) after HME to 4.7 ± 0.3% (3DP_2) and 4.8 ± 0.1% (3DP_5) after 3DP, with a layer thickness of 0.3 mm, when SUC and TRE were used, respectively (Fig. 3). This was attributed to the relatively high temperature during 3DP. Furthermore, as previously observed, a layer thickness of 0.1 mm is more damaging than of 0.3 mm (Fig. 3). This may be explained by the slower movement of the build platform. This slowness leads to an extended area of contact between the nozzle of the printer and the printed devices (Carlier et al., 2019).

Despite the addition of SUC or TRE, it was demonstrated that a significant increase in HMWS appeared after 3DP. Therefore, it was hypothesized that the addition of a hydrophobic amino acid such as LEU could enhance the stability of the loaded mAb. Both disaccharides have already been investigated with LEU to improve the mAb powder properties during the SD process. Combinations of stabilizers and LEU (5% w/w) have already been investigated and showed promising results on powder characteristics (Molina et al., 2017).

To improve the amorphous glassy state of the powder, a mixture of selected disaccharides (SUC and TRE) and LEU was investigated. It seemed interesting to promote this glassy state as it was expected to improve the stability of mAb. Indeed, TRE and LEU-based formulations have already been described as ensuring good protein stabilization by promoting this glassy state (Minne et al., 2008; Sou et al., 2015). Therefore, 3DP devices loaded with SUC-LEU and TRE-LEU were printed using a layer thickness of 0.3 mm.

To evaluate the potential benefit of the addition of LEU on the stability of the loaded mAb, HMWS levels were evaluated after each process (from spray drying to 3DP). After 3DP, these levels were 4.4 ± 0.2% and 3.6 ± 0.1% for 3DP_3 (SUC-LEU) and 3DP_6 (TRE-LEU), respectively (Fig. 3). These levels were compared to those obtained when SUC and TRE were used alone. It was demonstrated that the addition of LEU to SUC and TRE decreased the production of HMWS. However, the decrease in HMWS was significant only with the association of TRE-LEU (p-value < 0.0001). The rate of increase was compared as a ratio over the whole process (between 3DP and SD). Indeed, following the addition of LEU to TRE, the percentage of HMWS increased by about 18% versus 50% when TRE was formulated alone (Fig. 3). The same trend was observed when LEU was added to SUC with higher HMWS levels (SUC-LEU: 33% vs SUC: 66% increase) (Fig. 3).

LMWS levels after 3DP were then also investigated. A slight increase in LMWS (around 0.05 ± 0.04%) was demonstrated, regardless of whether LEU was added to SUC or TRE (data not shown).

Finally, drug loadings were assessed on 3DP DDS. The BCA results showed loadings close to the theoretical loading of 15% (w/w) (Table 3). These results were consistent with the loading of printable filaments. Thus, results were in phase with the previous statement about the uniform dispersion of mAb in the polymeric matrix expressed after HME.

To the best of our knowledge, there is no report of this manufacturing process, which uses mAb-loaded SD particles to extrude printable filaments by HME for use in FDM to create 3DP DDS. According to the previous results, the increase in HMWS was directly related to the thermal degradation occurring at 90 °C and 105 °C with HME and 3DP, respectively. However, it was shown that the formulation containing TRE-LEU was able to minimize the production of HMWS and to promote mAb stability. Therefore, this formulation was investigated through *in vitro* evaluations such as dissolution tests as well as the binding capacity evaluation. Indeed, the integrity of the mAb after its release form the DDS must be preserved.

3.5. Dissolution tests

It was previously demonstrated and described that PLGA-based DDS (e.g. microparticles and implants) are characterized by a triphasic release profiles. These phases include an initial burst effect (I), a latent phase with diffusion driven release (II) and a sustained release of the drug due to the erosion of the polymer (III) (Arrighi et al., 2019; Duque et al., 2018; Fredenberg et al., 2011). To ensure a steady and sustained release of the loaded mAb over time, melt processing such as 3DP seemed adequate. To our knowledge, systems such as microparticles have shown high burst effects (Arrighi et al., 2019; Marquette et al., 2014). This issue could be decreased using DDS with a dense polymer matrix.

The instability of a mAb increases in liquid state and may lead to chemical degradations (Angkawinitwong et al., 2015). Moreover, it could be interesting to promote a release profile where a limited latent phase occurs. Indeed, the latent phase could lead to mAb degradation due to its retention in the polymer matrix and the medium uptake. Moreover, a linear release profile which could tend towards a "zero order kinetic" should allow a constant drug release and a steady release concentration of the mAb in the dissolution medium.

The release of the mAb was characterized by a low burst effect 2.0 ± 0.3% within 24 h (Fig. 4a). Such low burst effect was already observed from PLGA-based formulations obtained by HME due to the monolithic

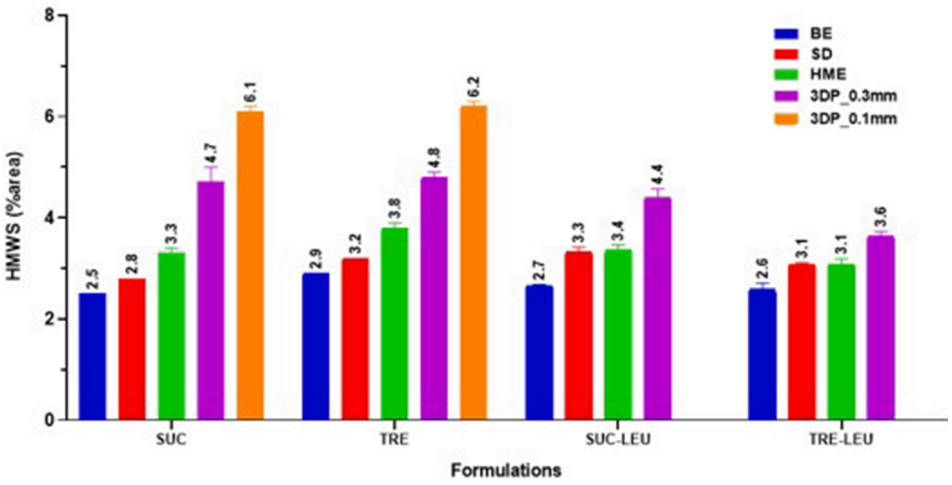

Fig. 3. Comparison of the HMWS levels for the mAb formulation (mAb:stabilizer ratio 2.0:1) containing SUC, TRE, SUC-LEU and TRE-LEU after BE, SD, HME and 3DP. Formulations are summarized as SUC: SD_16 (BE, SD), HME_16 (HME), 3DP_2 (3DP_0.3 mm) and 3DP_1 (3DP_0.1 mm); TRE: SD_18 (BE, SD), HME_18 (HME), 3DP_5 (3DP_0.3 mm) and 3DP_4 (3DP_0.1 mm); SUC-LEU: SD_17 (BE, SD), HME_17 (HME) and 3DP_3 (3DP_0.3 mm); TRE-LEU: SD_19 (BE, SD), HME_19 (HME) and 3DP_6 (3DP_0.3 mm) (Table 1).

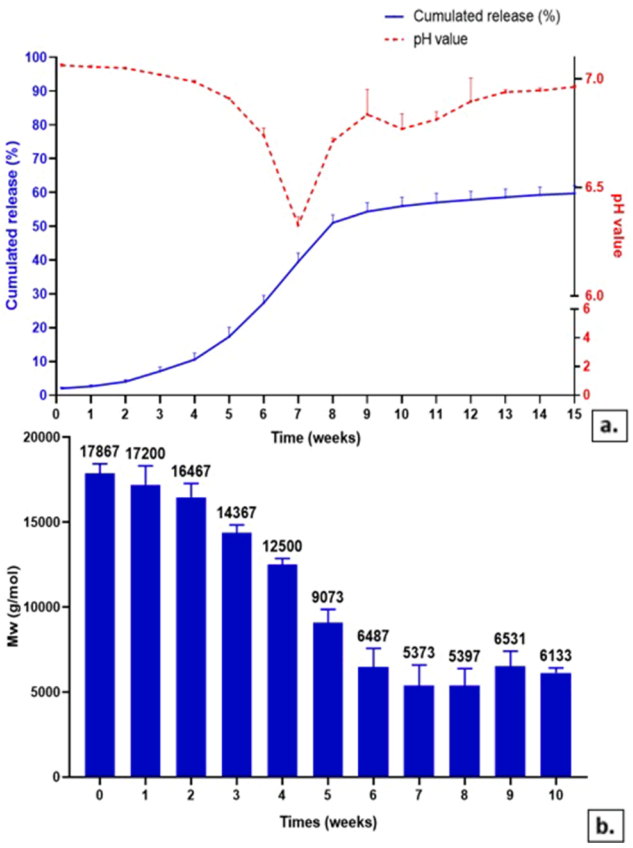

Fig. 4. (**a**) Dissolution profiles of 3DP DDS containing mAb stabilized with 3DP_17 TRELEU formulation (blue solid line) and varying *in vitro* pH values of the surrounding medium over dissolution time (red dashed line). (**b**) Degradation of the PLGA contained in 3DP DDS over 10 weeks in the dissolution medium at 37 °C.

(dense) matrix and the limited access of dissolution medium to extract the mAb (Lee and Pokorski, 2018). For instance, Cossé et al. reported a burst release after 24 h of 3.7 ± 0.2% from BSA-loaded PLGA implants produced by HME (Cossé et al., 2016).

The sustained release occurred over time starting with a slow release phase (latent phase) within the first weeks. Weeks 1 to 4 showed a low protein release of up to 10.6 ± 1.9% (Fig. 4a). This was due to the struggle of medium to penetrate the PLGA matrix and is known to be low during the first weeks. Water diffusion from the surface to the centre of the devices led to the swelling of PLGA (Bode et al., 2019; Cossé et al., 2016). An increase in the percentage of release of the mAb was then observed in the following weeks. The cumulative release accelerated and increased from 17.3 ± 2.8% after 5 weeks to 57.8 ± 2.5% after 12 weeks. Finally, a low release phase was observed to reach 59.7 ± 2.3% within 15 weeks (Fig. 3a).

The release of the mAb was dependent on the uptake of water, which allows mAb diffusion through the pores of the DDS. However, the diffusion from the dense PLGA matrix is promoted with its degradation to increase this porous network (Lee and Pokorski, 2018). Degradation of the RG502 was evaluated on the 3DP DDS during the dissolution test (Fig. 3b). PLGA was degraded by hydrolytic cleavage of its ester linkages which produces oligomers of PLGA and leads to erosion of the device (Hines and Kaplan, 2013). It has already been widely reported that the hydrolysis of PLGA acidifies the medium due to the release of PLA and PGA residues. Such acidification tends to induce an autocatalyze, which accelerates the hydrolysis of PLGA (Houchin et al., 2007). The diffusion of the medium through the polymeric matrix is needed to trigger the hydrolysis and promotes the erosion of the DDS (Cossé et al., 2016). Erosion is the diffusion of oligomers (or monomers) of PLGA from the matrix to the dissolution medium. The PLGA derivative, Resomer® RG502, was characterized with an initial Mw of 17 867 ± 577 g/mol. This result was consistent with the literature (Zlomke et al., 2019).

Initially, RG502 hydration occurred during the first weeks of the dissolution test. Water penetrates from the surface through the centre. Degradation of polymer was marginally observed, and the pH value of the surrounding medium remained constant (Fig. 4). Degradation then increased after 3 weeks with a loss of around 20% (14 367 ± 462 g/mol) of the RG502 initial mass. This loss was due to the hydrolytic scission of the RG502 in oligomers into the devices. Erosion started after 3 weeks, according to the decrease in pH value of the surrounding medium (Fig. 4a). This erosion is driven by the oligomers (or monomers) generated from the RG502 matrix. During the first weeks, mainly degradation occurred, but the onset of erosion was triggered and accelerated with the pH drop. Therefore, the autocatalysis accelerated the erosion and increased both PLGA degradation and mAb release. For instance, a loss of 64% (5373 ± 1217 g/mol) of the initial mass of the PLGA was observed after 7 weeks of dissolution (Fig. 4b). Interestingly, the pH value decreased to 6.3 ± 0.1%, which also demonstrated the highest rate of erosion. No further degradation was reported after this main degradation and the polymer Mw remained stable around 6 000 g/mol (Fig. 4b). Moreover, the erosion rate decreased after week 7. This statement was demonstrated by the increase in the pH value in the following weeks, from 6.7 ± 0.1% (week 8) to 7.0 ± 0.1% after 15 weeks (Fig. 4a). It was previously reported that erosion of an RG502 15% (w/w) BSA-loaded implant stopped after 7 weeks (50–60 days) (Cossé et al., 2016). Ghalanbor et al. demonstrated that incomplete erosion was correlated to an incomplete release of BSA (Ghalanbor et al., 2013). Therefore, the observation made from our 3DP mAb-loaded DDP was consistent with the literature. However, the release of the mAb was promoted within 15 weeks and the pH values remained slightly acidic due to the generation of oligomers and their diffusion into the dissolution medium. This diffusion may be due to the pore formation in the matrix and constant water penetration through the centre of the 3DP devices over time. Several phenomena (i.e. diffusion, erosion) occurred during the release mechanism and could evolve in phases from the surface towards the centre of the devices. No investigation of PLGA degradation longer than 10 weeks was shown. Indeed, the sample generated after 10 weeks in the dissolution medium remained insoluble in chloroform. PLGA and mAb may form insoluble aggregates over time. A similar observation has been reported in the literature and was explained by the formation of thioester bonds between BSA and the PLGA matrix (Ghalanbor et al., 2012). Furthermore, this observation was consistent with the low release phase observed after 10 weeks of dissolution and the incomplete mAb release after 15 weeks (Fig. 4a).

The sustained release of the mAb was demonstrated. However, the rehydration and the diffusion of the mAb in the dissolution medium led to mAb instabilities (Fig. 5). These instabilities were promoted by the aqueous medium and the decrease in the pH. This decrease may promote interactions between PLGA and mAb. Such decrease could impair the integrity of the mAb in the DDS. Indeed, it was previously demonstrated that the microenvironmental pH within a PLGA-based device led to the degradation of the loaded peptide (Liu et al., 2019; Schädlich et al., 2014). Therefore HMWS and LMWS levels as well as the monomer content were assessed during the dissolution test (Fig. 4a). As already mentioned, during its erosion, the PLGA-based matrix generates acidic species, which led to a decrease in the medium pH. This was needed to extract the entrapped mAb entity into the 3DP-device matrix during its quantification.

Thus, stability of the mAb was also assessed during the dissolution test. mAb integrity was evaluated after its release in the dissolution medium due to mAb monomers, as well as the increase in both HMWS and LMWS levels (Fig. 5). It was shown that a decrease in the monomer percentage was associated with an increase in either HMWS or LMWS species. Indeed, the mAb monomer corresponds to the functional Y-shaped structure and needs to be protected to extend the binding

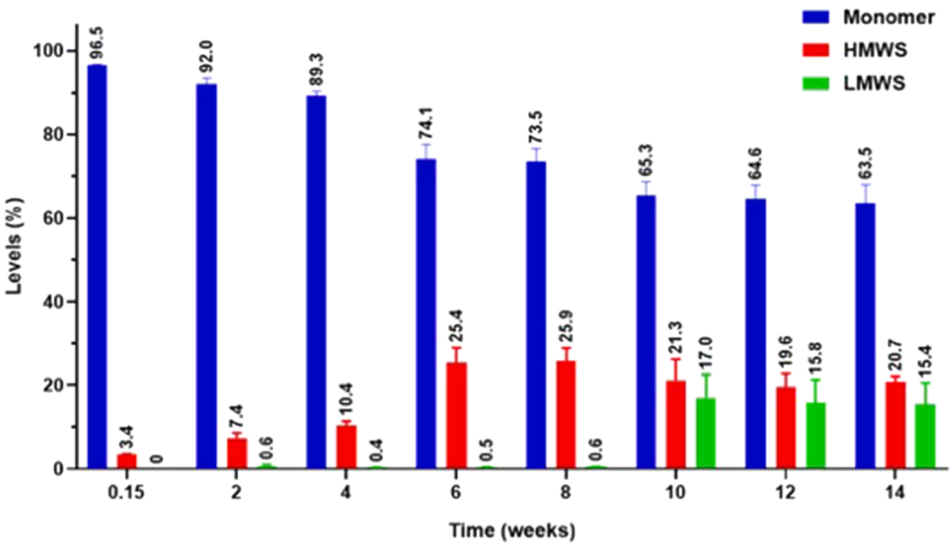

Fig. 5. Comparison of monomer, HMWS and LMWS levels (%) of the released mAb from 3DP_17 during the *in vitro* dissolution test. The mAb reference was characterized with 97.4 ± 0.4% (monomer), 2.6 ± 0.4% (HMWS) and no LMWS.

capacity and biological activity of the immunoglobulin.

The highest HMWS levels were observed between week 6 (25.4 ± 3.6%) and week 8 (25.9 ± 3.1%) (Fig. 5). This increase was correlated with the highest erosion rate, as previously discussed, and the decrease in the pH to 6.3 ± 0.1 at week 7 (Fig. 4a). Interestingly, a slight increase in LMWS was observed (<0.7%) during the first 9 weeks of dissolution. However, LMWS levels increased to 17.0 ± 5.7% after 10 weeks (Fig. 5). This level remained high, with a value of 15.4 ± 5.2% after 14 weeks (Fig. 5). The fragmentation was showed at a delayed stage of the dissolution test. It may be due to the hydration of the core of the PLGA-based devices, which occurred after the main erosion of the matrix. Therefore, the decrease in the pH, combined with the complexity of extracting the mAb from the core, appeared more deleterious than during the main erosion process. As shown by the pH value of 6.7 ± 0.1% (week 10), acidic species were still extracted from the matrix (Fig. 4a).

The monomer content reached 96.5 ± 0.3% after 24 h (burst effect) (Fig. 4). This showed a decrease over time due to the instabilities during the dissolution test. The monomer content decreased to 74.1 ± 3.6% and 64.6 ± 3.3% after 6 and 12 weeks, respectively (Fig. 5).

An ELISA test was finally performed to evaluate the binding capacity of mAb after its diffusion from the devices to the dissolution medium. Despite the decrease in the monomer content, it seemed interesting to evaluate the mAb binding to its target.

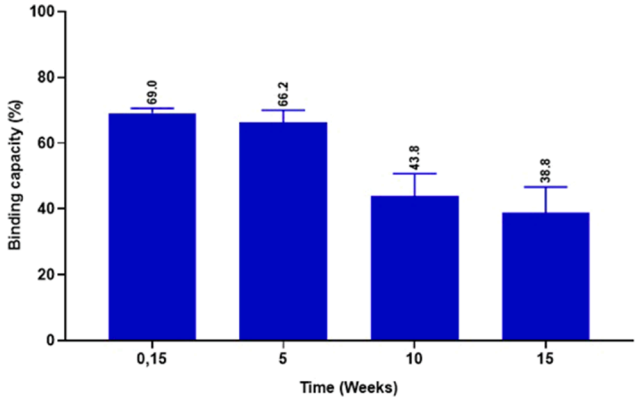

Fig. 6. Comparison of the binding capacity of the released mAb from 3DP_7 after 24 h, 5, 10 and 15 weeks of dissolution.

The binding capacity of mAb was found to be 69.0 ± 1.5% after 24 h (Fig. 6). This value was lower than expected from the low HMWS level and the high monomer content (96.5 ± 0.3%) previously observed (Fig. 5). Indeed, the monomer content was at its maximum after 24 h of dissolution. The binding capacity after 24 h could be directly associated with the degradation of mAb during the manufacturing process. A slight decrease in the binding capacity was demonstrated after 5 weeks (66.2 ± 3.8%) (Fig. 6). After 10 and 15 weeks, the binding capacity drastically decreased to 43.8 ± 6.8% and 38.8 ± 7.9%, respectively (Fig. 6). These low values may be due to the increase in the LMWS and HMWS levels, which impaired the affinity of the mAb after 10 weeks.

These results showed that complementary methods are needed to characterize the mAb integrity. It could be interesting to evaluate the secondary structure of the mAb using an analytical method such as circular dichroism. Indeed, it was reported that forced degradation at temperatures higher than 60 °C led to notable structural changes such as loss of β-sheet and unordered structures (Hermosilla et al., 2020).

4. Conclusion

Our results showed that the association of HME and an FDM 3D printer was suitable to produce mAb-loaded DDS with high drug loading (15% w/w). Homogeneous solid dispersion of the mAb in the PLGA matrix was reached in both printable filaments and 3DP DDS. Different stabilizers were investigated to stabilize the mAb against thermal degradation. Disaccharides (TRE and SUC) promoted mAb integrity during the spray drying, HME and 3DP steps using an mAb:stabilizer ratio of 2.0:1. The optimization of the formulation using a low amount of LEU allowed the stability of the mAb against potential thermal degradation to be improved. The association of mAb with TRE-LEU showed the lowest HMWS levels and no fragmentation was observed. The dissolution profile then showed an interesting sustained-release profile with a limited burst effect. Finally, it was demonstrated that, despite the relatively high temperatures of extrusion (90 °C) and printing (105 °C), mAb binding capacity of up to 70% was maintained after 24 h of dissolution. This observation was compared with the HMWS and LMWS levels during the mAb dissolution from the 3DP DDS. The monomer content demonstrated a value of 96.5 ± 0.3% after 24 h. Thus, complementary analytical methods may be necessary to understand how thermal stresses impair the mAb binding capacity. Further *in vivo* investigations may be useful to complete and correlate the *in vitro* data generated in this work.

CRediT authorship contribution statement

E. Carlier: Investigation, Formal analysis, Writing - original draft, Visualization. **S. Marquette:** Writing - review & editing, Resources, Supervision. **C. Peerboom:** Writing - review & editing, Resources. **K. Amighi:** Supervision, Writing - review & editing, Resources. **J. Goole:** Supervision, Validation, Writing - review & editing.

Declaration of Competing Interest

The authors declare that they have no known competing financial interests or personal relationships that could have appeared to influence the work reported in this paper.

Acknowledgements

The authors would like to thank UCB Pharma S.A. and the Walloon Region for providing the funding to make this study possible. They also wish to thank Giuseppe Manini for having performed GPC analysis at the Laboratory of Polymeric and Composite Materials of UMons (Dir. J-M Raquez, S. Benali). Finally, the authors would like to thank the Micro-milli platform of the Université libre de Bruxelles.

References

Afrose, M.F., Masood, S.H., Nikzad, M., Iovenitti, P., 2014. 1. Effects of build orientations on tensile properties of PLA material processed by FDM. Adv. Mater. Res. 1044–1045, 31–34. https://doi.org/10.4028/www.scientific.net/AMR.1044-1045.31.

Angkawinitwong, U., Sharma, G., Khaw, P.T., Brocchini, S., Williams, G.R., 2015. Solid-state protein formulations. Ther. Deliv. https://doi.org/10.4155/tde.14.98.

Arrighi, A., Marquette, S., Peerboom, C., Denis, L., Goole, J., Amighi, K., 2019. Development of PLGA microparticles with high immunoglobulin G-loaded levels and sustained-release properties obtained by spray-drying a water-in-oil emulsion. Int. J. Pharm. 566, 291–298. https://doi.org/10.1016/j.ijpharm.2019.05.070.

Awwad, S., Angkawinitwong, U., 2018. Overview of Antibody Drug Delivery. Pharmaceutics 10, 83. https://doi.org/10.3390/pharmaceutics10030083.

Azad, M.A., Olawuni, D., Kimbell, G., Badruddoza, A.Z.M., Hossain, M.S., Sultana, T., 2020. Polymers for extrusion-based 3D printing of pharmaceuticals: A holistic materials–process perspective. Pharmaceutics. https://doi.org/10.3390/pharmaceutics12020124.

Baek, Y., Singh, N., Arunkumar, A., Zydney, A.L., 2017. Effects of histidine and sucrose on the biophysical properties of a monoclonal antibody. Pharm. Res. 34, 629–639. https://doi.org/10.1007/s11095-016-2092-0.

Bode, C., Kranz, H., Fivez, A., Siepmann, F., Siepmann, J., 2019. Often neglected: PLGA/PLA swelling orchestrates drug release: HME implants. J. Control. Release 306, 97–107. https://doi.org/10.1016/j.jconrel.2019.05.039.

Bowen, M., Turok, R., Maa, Y.F., 2013. Spray drying of monoclonal antibodies: investigating powder-based biologic drug substance bulk storage. Dry. Technol. 31, 1441–1450. https://doi.org/10.1080/07373937.2013.796968.

Carlier, E., Marquette, S., Peerboom, C., Denis, L., Benali, S., Raquez, J.M., Amighi, K., Goole, J., 2019. Investigation of the parameters used in fused deposition modeling of poly(lactic acid) to optimize 3D printing sessions. Int. J. Pharm. 565, 367–377. https://doi.org/10.1016/j.ijpharm.2019.05.008.

Cicerone, M.T., Pikal, M.J., Qian, K.K., 2015. Stabilization of proteins in solid form. Adv. Drug Deliv. Rev. https://doi.org/10.1016/j.addr.2015.05.006.

Cossé, A., König, C., Lamprecht, A., Wagner, K.G., 2016. Hot melt extrusion for sustained protein release: matrix erosion and in vitro release of PLGA-based implants. AAPS PharmSciTech. https://doi.org/10.1208/s12249-016-0548-5.

Costa, S.F., Duarte, F.M., Covas, J.A., 2015. Thermal conditions affecting heat transfer in FDM/FFE: a contribution towards the numerical modelling of the process: This paper investigates convection, conduction and radiation phenomena in the filament deposition process. Virtual Phys. Prototyp. 10, 35–46. https://doi.org/10.1080/17452759.2014.984042.

Cummings, J.H., Stephen, A.M., 2007. Carbohydrate terminology and classification. Eur. J. Clin. Nutr. 61, S5–S18. https://doi.org/10.1038/sj.ejcn.1602936.

Duque, L., Körber, M., Bodmeier, R., 2018. Improving release completeness from PLGA-based implants for the acid-labile model protein ovalbumin. Int. J. Pharm. 538, 139–146. https://doi.org/10.1016/j.ijpharm.2018.01.026.

Fredenberg, S., Wahlgren, M., Reslow, M., Axelsson, A., 2011. The mechanisms of drug release in poly(lactic-co-glycolic acid)-based drug delivery systems–a review. Int. J. Pharm. 415, 34–52. https://doi.org/10.1016/j.ijpharm.2011.05.049.

Ghalanbor, Z., Körber, M., Bodmeier, R., 2013. Interdependency of protein-release completeness and polymer degradation in PLGA-based implants. Eur. J. Pharm. Biopharm. 85, 624–630. https://doi.org/10.1016/j.ejpb.2013.03.031.

Ghalanbor, Z., Körber, M., Bodmeier, R., 2012. Protein release from poly(lactide-co-glycolide) implants prepared by hot-melt extrusion: Thioester formation as a reason for incomplete release. Int. J. Pharm. 438, 302–306. https://doi.org/10.1016/j.ijpharm.2012.09.015.

Ghalanbor, Z., Körber, M., Bodmeier, R., 2010. Improved lysozyme stability and release properties of Poly(lactide-co- glycolide) implants prepared by hot-melt extrusion. Pharm. Res. 27, 371–379. https://doi.org/10.1007/s11095-009-0033-x.

Cicerone, M.T., Pikal, M.J., Qian, K.K., 2015. Stabilization of proteins in solid form. Adv. Drug Deliv. Rev. https://doi.org/10.1016/j.addr.2015.05.006.

Goyanes, A., Buanz, A.B.M., Hatton, G.B., Gaisford, S., Basit, A.W., 2015a. 3D printing of modified-release aminosalicylate (4-ASA and 5-ASA) tablets. Eur. J. Pharm. Biopharm. 89, 157–162. https://doi.org/10.1016/j.ejpb.2014.12.003.

Goyanes, A., Wang, J., Buanz, A., Martínez-Pacheco, R., Telford, R., Gaisford, S., Basit, A. W., 2015b. 3D printing of medicines: engineering novel oral devices with unique design and drug release characteristics. Mol. Pharm. 12, 4077–4084. https://doi.org/10.1021/acs.molpharmaceut.5b00510.

Hermosilla, J., Pérez-Robles, R., Salmerón-García, A., Casares, S., Cabeza, J., Bones, J., Navas, N., 2020. Comprehensive biophysical and functional study of ziv-aflibercept: characterization and forced degradation. Sci. Rep. 10 https://doi.org/10.1038/s41598-020-59465-7.

Hines, D.J., Kaplan, D.L., 2013. Poly(lactic-co-glycolic) acid-controlled-release systems: experimental and modeling insights. Crit. Rev. Ther. Drug Carrier Syst. 30, 257–276. https://doi.org/10.1615/2013006475.

Holländer, J., Genina, N., Jukarainen, H., Khajeheian, M., Rosling, A., M??kil??, E., Sandler, N., 2016. Three-dimensional printed PCL-based implantable prototypes of medical devices for controlled drug delivery. J. Pharm. Sci. 105, 2665–2676. https://doi.org/10.1016/j.xphs.2015.12.012.

Houchin, M.L., Neuenswander, S.A., Topp, E.M., 2007. Effect of excipients on PLGA film degradation and the stability of an incorporated peptide. J. Control. Release 117, 413–420. https://doi.org/10.1016/j.jconrel.2006.11.023.

Jain, N.K., Roy, I., 2009. Effect of trehalose on protein structure. Protein Sci. https://doi.org/10.1002/pro.3.

Jamróz, W., Szafraniec, J., Kurek, M., Jachowicz, R., 2018. 3D printing in pharmaceutical and medical applications – recent achievements and challenges, pharmaceutical research. Springer New York LLC. https://doi.org/10.1007/s11095-018-2454-x.

Kamerzell, T.J., Esfandiary, R., Joshi, S.B., Middaugh, C.R., Volkin, D.B., 2011. Protein-excipient interactions: Mechanisms and biophysical characterization applied to protein formulation development. Adv. Drug Deliv. Rev. https://doi.org/10.1016/j.addr.2011.07.006.

Kanojia, G., Have, R. Ten, Bakker, A., Wagner, K., Frijlink, H.W., Kersten, G.F.A., Amorij, J.P., 2016. The production of a stable Infliximab powder: The evaluation of spray and freeze-drying for production. PLoS ONE 11. https://doi.org/10.1371/journal.pone.0163109.

Kollamaram, G., Croker, D.M., Walker, G.M., Goyanes, A., Basit, A.W., Gaisford, S., 2018. Low temperature fused deposition modeling (FDM) 3D printing of thermolabile drugs. Int. J. Pharm. 545, 144–152. https://doi.org/10.1016/j.ijpharm.2018.04.055.

Le Basle, Y., Chennell, P., Tokhadze, N., Astier, A., Sautou, V., 2020. Physicochemical stability of monoclonal antibodies: a review. J. Pharm. Sci. https://doi.org/10.1016/j.xphs.2019.08.009.

Lee, P.W., Pokorski, J.K., 2018. Poly(lactic-co-glycolic acid) devices: Production and applications for sustained protein delivery. Wiley Interdiscip. Rev. Nanomedicine Nanobiotechnology 10, e1516. https://doi.org/10.1002/wnan.1516.

Ligon, S.C., Liska, R., Stampfl, J., Gurr, M., Mülhaupt, R., 2017. Polymers for 3D printing and customized additive manufacturing, chemical reviews. Am. Chem. Soc. https://doi.org/10.1021/acs.chemrev.7b00074.

Liu, J., Xu, Y., Wang, Y., Ren, H., Meng, Z., Liu, K., Liu, Z., Huang, H., Li, X., 2019. Effect of inner pH on peptide acylation within PLGA microspheres. Eur. J. Pharm. Sci. 134, 69–80. https://doi.org/10.1016/j.ejps.2019.04.017.

Luebbert, C., Huxoll, F., Sadowski, G., Van Den Mooter, G., Grohganz, H., 2017. Amorphous-amorphous phase separation in API/polymer formulations. Molecules 22, 296. https://doi.org/10.3390/molecules22020296.

Marquette, S., Peerboom, C., Yates, A., Denis, L., Goole, J., Amighi, K., 2014. Encapsulation of immunoglobulin G by solid-in-oil-in-water: Effect of process parameters on microsphere properties. Eur. J. Pharm. Biopharm. 86, 393–403. https://doi.org/10.1016/j.ejpb.2013.10.013.

Maury, M., Murphy, K., Kumar, S., Mauerer, A., Lee, G., 2005. Spray-drying of proteins: Effects of sorbitol and trehalose on aggregation and FT-IR amide I spectrum of an immunoglobulin G. Eur. J. Pharm. Biopharm. 59, 251–261. https://doi.org/10.1016/j.ejpb.2004.07.010.

Melocchi, A., Parietti, F., Loreti, G., Maroni, A., Gazzaniga, A., Zema, L., 2015. 3D printing by fused deposition modeling (FDM) of a swellable/erodible capsular device for oral pulsatile release of drugs. J. Drug Deliv. Sci. Technol. 30, 360–367. https://doi.org/10.1016/j.jddst.2015.07.016.

Mensink, M.A., Frijlink, H.W., van der Voort Maarschalk, K., Hinrichs, W.L.J., 2017. How sugars protect proteins in the solid state and during drying (review): Mechanisms of stabilization in relation to stress conditions. Eur. J. Pharm. Biopharm. https://doi.org/10.1016/j.ejpb.2017.01.024.

Minne, A., Boireau, H., Horta, M.J., Vanbever, R., 2008. Optimization of the aerosolization properties of an inhalation dry powder based on selection of excipients. Eur. J. Pharm. Biopharm. 70, 839–844. https://doi.org/10.1016/j.ejpb.2008.06.013.

Mensink, M.A., Frijlink, H.W., van der Voort Maarschalk, K., Hinrichs, W.L.J., 2017. How sugars protect proteins in the solid state and during drying (review): Mechanisms of stabilization in relation to stress conditions. Eur. J. Pharm. Biopharm. https://doi.org/10.1016/j.ejpb.2017.01.024.

Norman, J., Madurawe, R.D., Moore, C.M.V., Khan, M.A., Khairuzzaman, A., 2017. A new chapter in pharmaceutical manufacturing: 3D-printed drug products. Adv. Drug Deliv. Rev. 108, 39–50. https://doi.org/10.1016/j.addr.2016.03.001.

Nowak, C., Cheung, J.K., Dellatore, S.M., Katiyar, A., Bhat, R., Sun, J., Ponniah, G., Neill, A., Mason, B., Beck, A., Liu, H., K. Cheung, J., M. Dellatore, S., Katiyar, A., Bhat, R., Sun, J., Ponniah, G., Neill, A., Mason, B., Beck, A., Liu, H., 2017. Forced degradation of recombinant monoclonal antibodies: A practical guide, mAbs. Taylor and Francis Inc. https://doi.org/10.1080/19420862.2017.1368602.

Ohtake, S., Kita, Y., Arakawa, T., 2011. Interactions of formulation excipients with proteins in solution and in the dried state. Adv. Drug Deliv. Rev. https://doi.org/10.1016/j.addr.2011.06.011.

Piedmonte, D.M., Hair, A., Baker, P., Brych, L., Nagapudi, K., Lin, H., Cao, W., Hershenson, S., Ratnaswamy, G., 2015. Sorbitol crystallization-induced aggregation in frozen mAb formulations. J. Pharm. Sci. 104, 686–697. https://doi.org/10.1002/jps.24141.

Pietrzak, K., Isreb, A., Alhnan, M.A., 2015. A flexible-dose dispenser for immediate and extended release 3D printed tablets. Eur. J. Pharm. Biopharm. 96, 380–387. https://doi.org/10.1016/j.ejpb.2015.07.027.

Pignatello, R., Cenni, E., Micieli, D., Fotia, C., Salerno, M., Granchi, D., Avnet, S., Sarpietro, M.G., Castelli, F., Baldini, N., 2009. A novel biomaterial for osteotropic drug nanocarriers: Synthesis and biocompatibility evaluation of a PLGA-ALE conjugate. Nanomedicine 4, 161–175. https://doi.org/10.2217/17435889.4.2.161.

Rajagopal, K., Wood, J., Tran, B., Patapoff, T.W., Nivaggioli, T., 2013. Trehalose limits BSA aggregation in spray-dried formulations at high temperatures: Implications in preparing polymer implants for long-term protein delivery. J. Pharm. Sci. 102, 2655–2666. https://doi.org/10.1002/jps.23634.

Schädlich, A., Kempe, S., Mäder, K., 2014. Non-invasive in vivo characterization of microclimate pH inside in situ forming PLGA implants using multispectral fluorescence imaging. J. Control. Release 179, 52–62. https://doi.org/10.1016/j.jconrel.2014.01.024.

Serno, T., Geidobler, R., Winter, G., 2011. Protein stabilization by cyclodextrins in the liquid and dried state. Adv. Drug Deliv. Rev. https://doi.org/10.1016/j.addr.2011.08.003.

Shah, S., Maddineni, S., Lu, J., Repka, M.A., 2013. Melt extrusion with poorly soluble drugs. Int. J. Pharm. https://doi.org/10.1016/j.ijpharm.2012.11.001.

Sou, T., Morton, D.A., Williamson, M., Meeusen, E.N., Kaminskas, L.M., McIntosh, M.P., 2015. Spray-dried influenza antigen with trehalose and leucine produces an aerosolizable powder vaccine formulation that induces strong systemic and mucosal immunity after pulmonary administration. J. Aerosol Med. Pulm. Drug Deliv. 28, 361–371. https://doi.org/10.1089/jamp.2014.1176.

Stewart, S.A., Domínguez-Robles, J., McIlorum, V.J., Mancuso, E., Lamprou, D.A., Donnelly, R.F., Larrañeta, E., 2020. Development of a biodegradable subcutaneous implant for prolonged drug delivery using 3D printing. Pharmaceutics 12, 105. https://doi.org/10.3390/pharmaceutics12020105.

Tiwari, R.V., Patil, H., Repka, M.A., 2016. Contribution of hot-melt extrusion technology to advance drug delivery in the 21st century. Expert Opin. Drug Deliv. 13, 451–464. https://doi.org/10.1517/17425247.2016.1126246.

Tonnis, W.F., Mensink, M.A., De Jager, A., Van Der Voort Maarschalk, K., Frijlink, H.W., Hinrichs, W.L.J., 2015. Size and molecular flexibility of sugars determine the storage stability of freeze-dried proteins. Mol. Pharm. 12, 684–694. https://doi.org/10.1021/mp500423z.

Wang, W., Singh, S., Zeng, D.L., King, K., Nema, S., 2007. Antibody structure, instability, and formulation. J. Pharm. Sci. https://doi.org/10.1002/jps.20727.

Zhang, J., Feng, X., Patil, H., Tiwari, R.V., Repka, M.A., 2017. Coupling 3D printing with hot-melt extrusion to produce controlled-release tablets. Int. J. Pharm. 519, 186–197. https://doi.org/10.1016/j.ijpharm.2016.12.049.

Zlomke, C., Barth, M., Mäder, K., 2019. Polymer degradation induced drug precipitation in PLGA implants – Why less is sometimes more. Eur. J. Pharm. Biopharm. 139, 142–152. https://doi.org/10.1016/j.ejpb.2019.03.016.